Virulence evolution in the opportunistic bacterial pathogen *Pseudomonas aeruginosa*

Short Title: Virulence evolution in an opportunistic pathogen

Elisa T. Granato[1,2]*, Christoph Ziegenhain[3,4], Rasmus L. Marvig[5], Rolf Kümmerli[1]*

[1]Department of Plant and Microbial Biology, University of Zurich, Zurich, Switzerland.

[2]Department of Zoology, University of Oxford, Oxford, United Kingdom.

[3]Department Biology II, Ludwig-Maximilians-University, Munich, Germany.

[4]Department of Cell and Molecular Biology, Karolinska Institutet, Stockholm, Sweden.

[5]Center for Genomic Medicine, Rigshospitalet, Copenhagen, Denmark.

*Correspondence to: Elisa T. Granato, elisa.granato@zoo.ox.ac.uk

Rolf Kümmerli, rolf.kuemmerli@uzh.ch

ABSTRACT

Bacterial opportunistic pathogens are feared for their difficult-to-treat nosocomial infections and for causing morbidity in immunocompromised patients. Here, we study how such a versatile opportunist, *Pseudomonas aeruginosa*, adapts to conditions inside and outside its model host *Caenorhabditis elegans*, and use phenotypic and genotypic screens to identify the mechanistic basis of virulence evolution. We found that virulence significantly dropped in unstructured environments both in the presence and absence of the host, but remained unchanged in spatially structured environments. The observed virulence decline was driven by a substantial reduction in the production of multiple virulence factors, including siderophores, toxins, and proteases. Because these virulence factors are secreted, we argue that the spread of non-producers is at least partially due to cheating, where mutants exploit the shareable virulence factors produced by the wildtype. Whole-genome sequencing of evolved clones revealed positive selection and parallel evolution across replicates, and showed an accumulation of mutations in regulator genes, controlling the expression of these virulence factors. Our study identifies the spatial structure of the non-host environment as a key driver of virulence evolution in an opportunistic pathogen, and indicates that disrupting spatial structure in chronic infections could steer pathogen evolution towards lower virulence.

INTRODUCTION

Understanding how microbial pathogens evolve is essential to predict their epidemiological spread through host populations and the damage they can inflict on host individuals. Evolutionary theory offers a number of concepts aiming at forecasting the evolution of pathogen virulence and identifying the key factors driving virulence evolution [1,2]. While most evolutionary models agree that the spatial structure of the environment is an important determinant of virulence evolution, they differ on whether spatial structure should boost or curb pathogen virulence. One set of models predicts that high spatial structure lowers virulence, because it favors clonal infections and thereby limits the risk of hosts being infected by multiple competing pathogen lineages [3–6]. In this scenario, it is thought that within clonal infections, the interests of pathogen individuals are aligned, which should select for prudent host exploitation and thus low virulence [7,8]. Another set of models predicts that high spatial structure increases virulence because it favors the cooperative secretion of harmful virulence factors required for successful host colonization [5,9,10]. These models are based on the idea that virulence factors, such as toxins, proteases and iron-scavenging siderophores, are shared between pathogen individuals in infections [11–13]. Hence, low spatial structure is predicted to favor the evolution of cheating mutants that exploit the virulence factors produced by others, without contributing themselves [14]. Invasions of these cheats would then lower overall virulence factor availability and damage to the host [15–19].

Both classes of models have received some empirical support. While experimental evolution studies with viruses showed that limited dispersal indeed favors more benign pathogens [20–22], work with bacteria showed evidence for the opposite pattern [17,23,24]. Although pioneering in

their own right, several fundamental questions have remained unaddressed so far. For one thing, the mechanistic basis of virulence evolution has often remained elusive [8,20,21,25]. Moreover, bacterial studies were mainly based on controlled mixed versus mono-infections using wildtype strains and engineered mutants deficient for virulence factor production. It thus remains unknown whether virulence-factor deficient mutants would indeed evolve *de novo* under low spatial structure and spread to high frequency. Finally, the bacterial studies used opportunistic pathogens, which were however generally directly transferred from host to host, thereby ruling out the possibility of these opportunists to adapt to the non-host environment, a factor that might clearly affect virulence evolution [26–28].

Here we aim to tackle these unaddressed issues by conducting an experimental evolution study, where we (i) allow opportunistic bacterial pathogens to adapt both to the host and the non-host environment, (ii) manipulate the spatial structure of the environment, and (iii) uncover the targets of selection and mechanisms provoking virulence change using high-throughput phenotypic screening combined with whole-genome sequencing of evolved clones. For our approach, we used the opportunistic human pathogen *Pseudomonas aeruginosa* infecting its model host, the nematode *Caenorhabditis elegans* [29,30]. This bacterium is typically acquired by the host from an environmental reservoir [31,32], and nematodes can quickly become infected through the intestinal tract because they naturally feed on bacteria [33]. In our experiment, we let *P. aeruginosa* PAO1 wildtype bacteria evolve for 60 days in four different environments in eight-fold replication, implementing a 2x2 full factorial design (Fig. 1A). To assess the role of spatial structure of the environment (first factor) for virulence evolution, we let the pathogens evolve in either unstructured uniform liquid or spatially structured solid medium. To understand how adaptation

to the non-host environment affects virulence within the host, we further let the pathogens evolve both in the presence and the absence of the host (second factor). Following evolution, we quantified changes in pathogenicity for each independent replicate, and assessed whether these changes are associated with alterations in the expression of four important virulence factors of *P. aeruginosa*, which include the siderophore pyoverdine, the toxin pyocyanin, secreted proteases, and the ability to form biofilms. Finally, we whole-genome sequenced 140 evolved clones to map phenotypes to genotypes, and to test for positive selection, parallel evolution among independent replicates, and orders of mutations during evolution.

RESULTS

Selection for reduced virulence in environments with low spatial structure

Prior to experimental evolution, we found that the ancestral wildtype was highly virulent by killing 76.2% and 83.9% of all host individuals within 24 hours in liquid and on solid media, respectively (Table S1). This pattern changed during evolution in spatially unstructured environments, where virulence dropped by 32.3% and 44.7% for populations that evolved with and without hosts, respectively (Fig. 1B+C, Fig. S1). Conversely, virulence remained high in structured environments. Overall, there was a significant effect of spatial structure on virulence evolution (linear mixed model: $df_{structure} = 24.7$, $t_{structure} = -2.11$, $p_{structure} = 0.045$), while host presence did not seem to matter ($df_{host} = 18.6$, $t_{host} = 0.86$, $p_{host} = 0.40$).

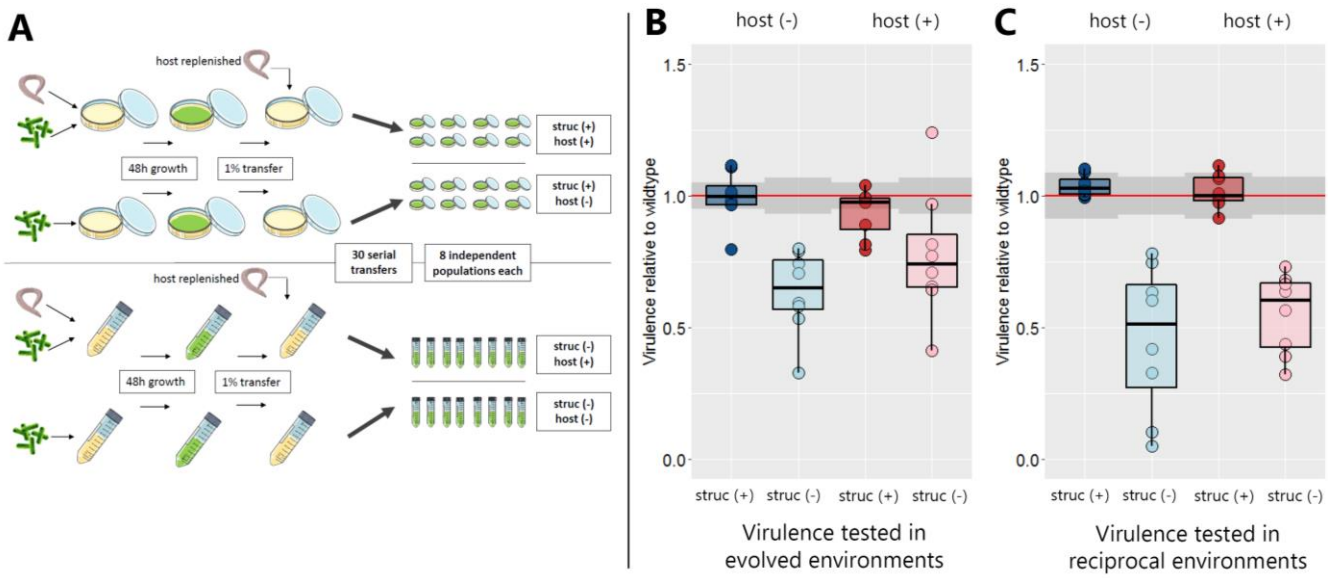

97

98 **Fig. 1. Virulence decreased during evolution in spatially unstructured environments.** (**A**)
99 Experimental design: *P. aeruginosa* PAO1 bacteria were serially transferred 30 times in four different
100 environments in 8-fold replication. These environments were either spatially structured ("struc +") or
101 unstructured ("struc −"), and either contained ("host +") or did not contain ("host −") *C. elegans* nematodes
102 for the bacteria to infect. Subsequently, the evolved populations were tested for their virulence towards the
103 nematode under two different conditions: (**B**) In the environment the populations evolved in (i.e.
104 populations that evolved on agar plates tested on agar plates, populations that evolved in liquid culture
105 tested in liquid culture); and (**C**) in the reciprocal environment as a control (populations that evolved on
106 agar plates tested in liquid culture, populations that evolved in liquid tested on agar plates). Both assays
107 revealed that virulence significantly decreased during evolution in unstructured environments (Wilcoxon
108 rank-sum test, $p < 0.05$; see Table S2). Virulence was quantified as percent nematodes killed at 24 h post
109 infection, scaled to the ancestral wildtype. Individual dots represent mean virulence of evolved populations.
110 The red line represents the average wildtype virulence level in the respective assay, with shaded areas
111 denoting the 95% confidence intervals.

112 *Treatment-specific changes in virulence factor production*

113 To explore whether shareable virulence factors were under selection and whether changes in
114 virulence factor production could explain the evolution of virulence, we isolated 640 evolved
115 clones and quantified their production of: (i) pyoverdine, required for iron-scavenging [34]; (ii)
116 pyocyanin, a broad-spectrum toxin [35]; and (iii) proteases to digest extracellular proteins [36].
117 We further quantified the pathogens' ability to form biofilms on surfaces, another social trait
118 typically involved with virulence [37]. We focussed on these four virulence-related traits because
119 of their demonstrated relevance in the *C. elegans* infection model [30,38–40].

120

121 Our phenotype screens revealed significant changes in the production of all four virulence factors
122 (Fig. 2). For pyoverdine, we observed a significant decrease in pyoverdine production in
123 unstructured environments without hosts, with many clones (44.4%) having completely lost the
124 ability to produce pyoverdine (Fig. 2A). Since our media was iron-limited, impeding the growth
125 of pyoverdine non-producers, these mutants likely represent social cheaters, exploiting the
126 pyoverdine secreted by producers [41,42]. While mutants with abolished pyoverdine production
127 also emerged in the unstructured environment with hosts, their frequency was much lower
128 (5.0%). Apart from the unstructured environment without hosts, we observed a significant
129 increase in pyoverdine production in evolved clones in all other treatments (Bayesian
130 generalized linear mixed model, BGLMM: $p_{\text{host:structure}} = 0.027$).

131

132 Pyocyanin production, meanwhile, significantly dropped in all four environments (Fig. 2B), but
133 more so in the presence than in the absence of the host ($p_{\text{host}} = 0.038$), while spatial structure
134 had no effect ($p_{\text{structure}} = 0.981$). The pattern of evolved protease production mirrored the one for

pyocyanin (Fig. 2C): there was a significant overall decrease in protease production, with a significant host (p_{host} = 0.042), but no structure ($p_{structure}$ = 0.489) effect. Since neither pyocyanin nor proteases are necessary for growth in our media, consisting of a protein-digest, reduced expression could reflect selection against dispensable traits. During infections, however, these traits are known to be beneficial [38,40] and accelerated loss could thus be explained by cheating, as secreted virulence factors could become exploitable inside the host. It is known that protease production can be exploited by non-producing clones [36], and there is recent evidence that the same might apply to pyocyanin [43].

Finally, the clones' ability to form surface-attached biofilms significantly increased in the presence of the host (p_{host} = 0.007) and in structured environments ($p_{structure}$ = 0.010), but decreased in the host-free unstructured environment (Fig. 2D). These findings indicate that attachment ability might be superfluous under shaken conditions, but could become important within the host to increase residence time.

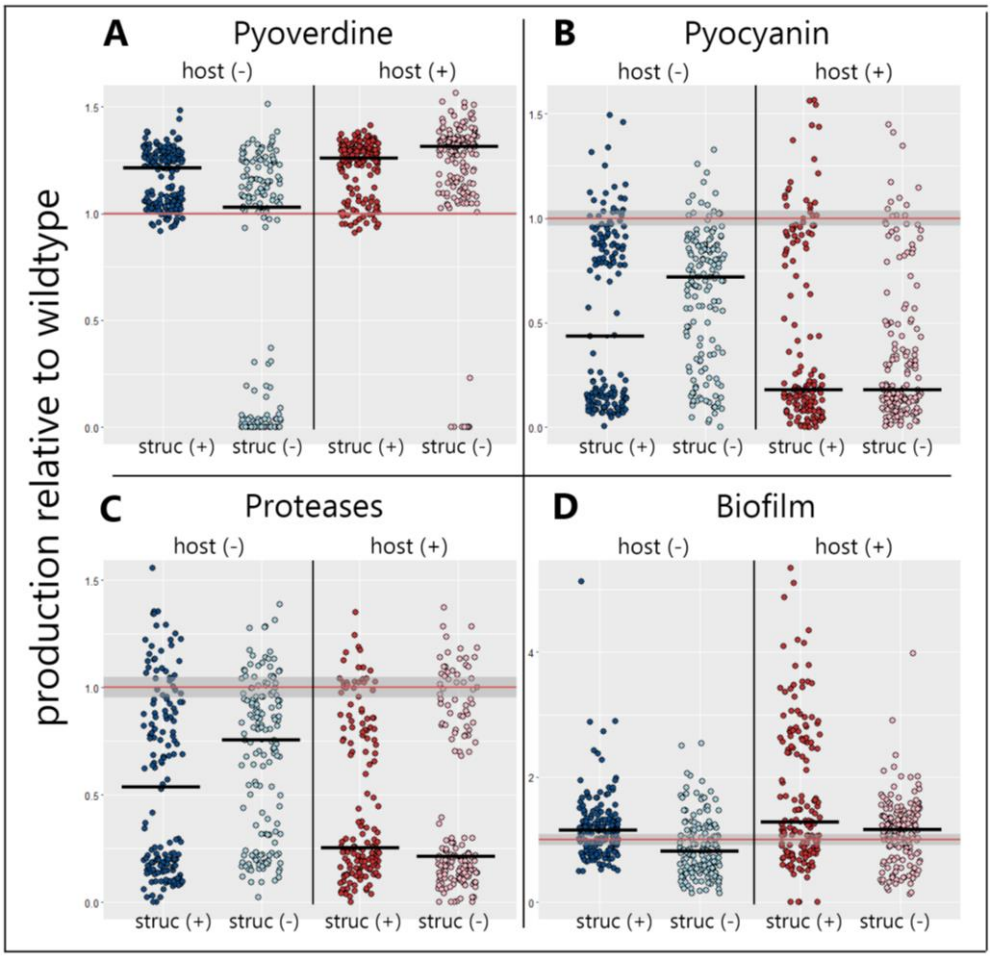

Fig. 2. **Selection promoted shifts in virulence factor production during experimental evolution.** The production levels of four important virulence factors were determined for 640 evolved *P. aeruginosa* clones (20 clones per evolved line), and compared to the ancestral wildtype (mean ± 95 % confidence intervals indicated as red lines and shaded areas, respectively). (**A**) The production of the siderophore pyoverdine significantly decreased in the host-free unstructured environment, but significantly increased in all other environments. (**B**) The production of the toxin pyocyanin significantly decreased in all environments, but more so in the environments with the host. (**C**) The production of proteases also significantly decreased in all environments, with a sharper decline in environments with the host. (**D**) The clones' ability to form surface-attached biofilms significantly decreased in the unstructured host-free environment, but significantly increased in all other environments. host (—) = host was absent during evolution; host (+) = host was present during evolution; struc (—) = evolution in a liquid-shaken unstructured environment; struc (+) = evolution in a structured environment on agar. We used non-parametric Wilcoxon rank-sum test for comparisons relative to the ancestral wildtype, and Bayesian-based generalized linear mixed models to test for treatment effects (see Table S2). Solid black bars denote the median for each treatment.

Aggregate change in virulence factor production correlates with evolved virulence

While the phenotypic screens revealed altered virulence factor production levels, with significant host and environmental effects (Fig. 2), the virulence data suggest that there is no host effect, and spatial structure is the only determinant of virulence evolution (Fig 1). In the attempt to reconcile these apparently conflicting results, we first performed a principle component analysis (PCA) on population averages of the four virulence factor phenotypes (Fig. 3A). The PCA indicates that each treatment evolved in a different direction in the phenotype space, revealing that environmental and host factors indeed both seem to matter. This analysis further shows that the direction of phenotypic changes was aligned for some traits, but opposed for others (Fig. 3A, Fig. S2A-F). A decrease in pyocyanin production was generally connected to a decrease in protease production (Fig. S2D). On the other hand, decreased pyocyanin and protease production was associated with both higher pyoverdine and biofilm production (Fig. S2B+E).

Given these opposing evolutionary directions and trade-offs between virulence factors we hypothesized that an increase in the production of one virulence factor could (at least partially) be counterbalanced by the reduction of another virulence factor. In the extreme case, two virulence factors could both be under selection, but in opposite directions, such that their net effects on virulence could cancel out. In line with this hypothesis, we found that the evolutionary change in virulence could only be explained when considering the aggregate change of all virulence factor phenotypes (Fig. 3B, $R^2 = 0.33$, $F(1,30) = 14.7$, $p < 0.001$; also see Fig. S4), but not when focussing on single virulence factors (Fig. S3). Thus, decreased virulence in unstructured environments is attributable to a simultaneous decrease in the production of multiple virulence factors (i.e. pyocyanin, proteases, and sometimes pyoverdine). Conversely, unchanged

187 virulence in structured environments can be explained by compensatory effects (i.e. the
188 reduction in pyocyanin and protease production is balanced by increased pyoverdine and
189 biofilm production). Important to note is that the observed pyoverdine upregulation is
190 presumably a compensatory phenotypic response, as decreased pyocyanin and protease
191 production are known to lower iron availability [44], which in turn might trigger increased
192 pyoverdine production.

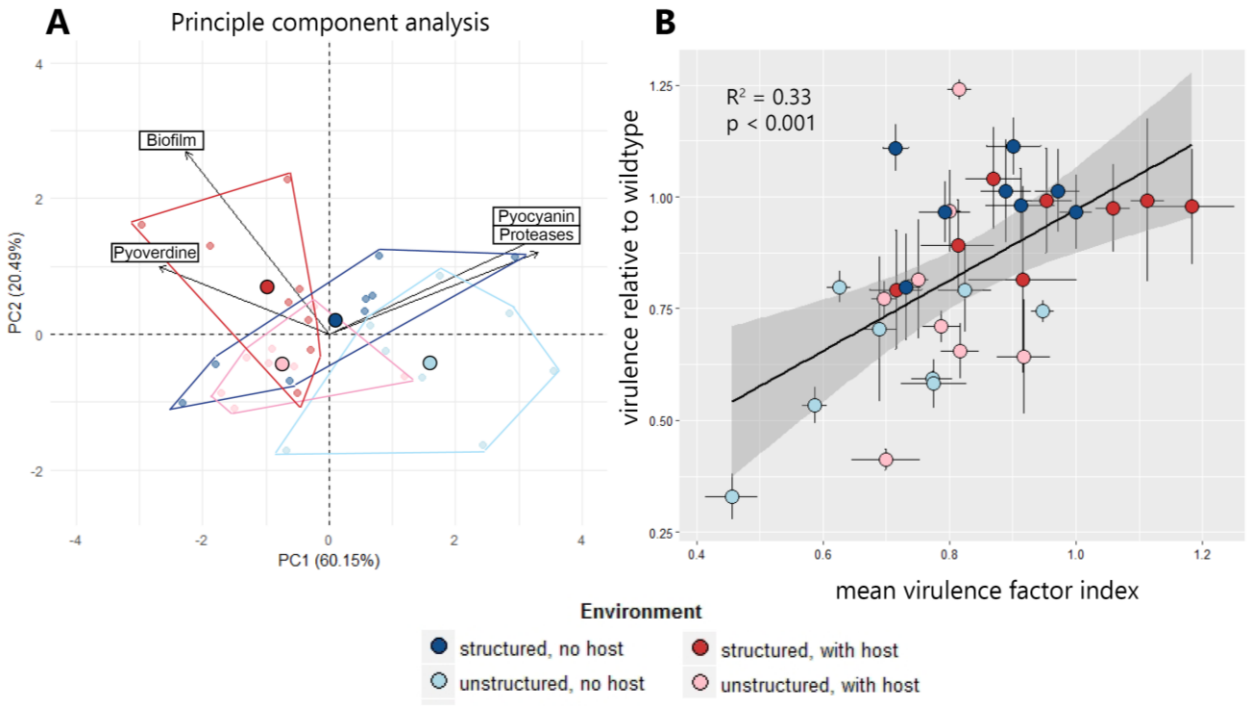

193

194 **Fig. 3. The aggregate change in virulence factor production explains virulence evolution.** (**A**) A
195 principle component analysis (PCA) on the population-level changes in the production of four virulence
196 factors (pyoverdine, pyocyanin, proteases, biofilm) reveals divergent evolutionary patterns. For instance,
197 analysis of the first two principal components (explaining 80.6 % of the total variance) shows complete
198 segregation between populations evolved in unstructured host-free environments and structured
199 environments with the host. Moreover, the PCA reveals that evolutionary change was aligned for some
200 traits (aligned vectors for pyocyanin and proteases), but opposed for others (inversed vectors for pyoverdine
201 versus pyocyanin/proteases). Small and large symbols depict individual population values and average
202 values per environment, respectively. Polygons show the boundaries in phenotype space for each
203 environment. (**B**) We found that the aggregate change in the production of all four virulence factors
204 explained the evolution of virulence. To account for the aligned and opposing effects revealed by the PCA,
205 we defined the "virulence factor index" as the average change in virulence factor production across all four
206 traits, scaled relative to the ancestral wildtype. Symbols and error bars depict mean values per population
207 and standard errors of the mean, respectively.

208 *Mutations in key regulators explain changes in virulence factor phenotypes*

209 To examine whether genetic changes can explain the observed shifts in virulence factor
210 production, we successfully sequenced the genome of 140 evolved clones from 16 independent
211 populations and compared them to the ancestor. Relative to the ancestral wildtype, we identified
212 182 mutations (153 SNPs and 29 microindels, i.e. small insertions and deletions), with 5-49
213 mutations per population (median = 8.5). Individual clones accumulated 0-5 mutations, except for
214 one clone (PA-030) with 42 mutations, of which 41 mutations were in a 5022 bp Pf1 prophage
215 region, a known mutational hotspot [45].

216

217 We identified 18 loci (genes and intergenic regions) that were independently mutated in at least
218 two populations (Fig. 4A). The most frequently mutated gene was *lasR*, encoding the regulator of
219 the Las quorum-sensing (QS) system. The second most frequent mutational target were ten
220 different *pil* genes, involved in type IV pili biosynthesis and twitching motility. The frequent
221 mutations in this cluster suggest that mutations in any of these genes could potentially lead to a
222 similar beneficial phenotype. Finally, the *pvdS* coding region or the *pvdG-pvdS* intergenic region,
223 containing the *pvdS* promoter, were also often mutated (i.e. in five populations). PvdS is the iron-
224 starvation sigma factor controlling pyoverdine synthesis, and mutations in this gene can lead to
225 pyoverdine deficiency [19,42].

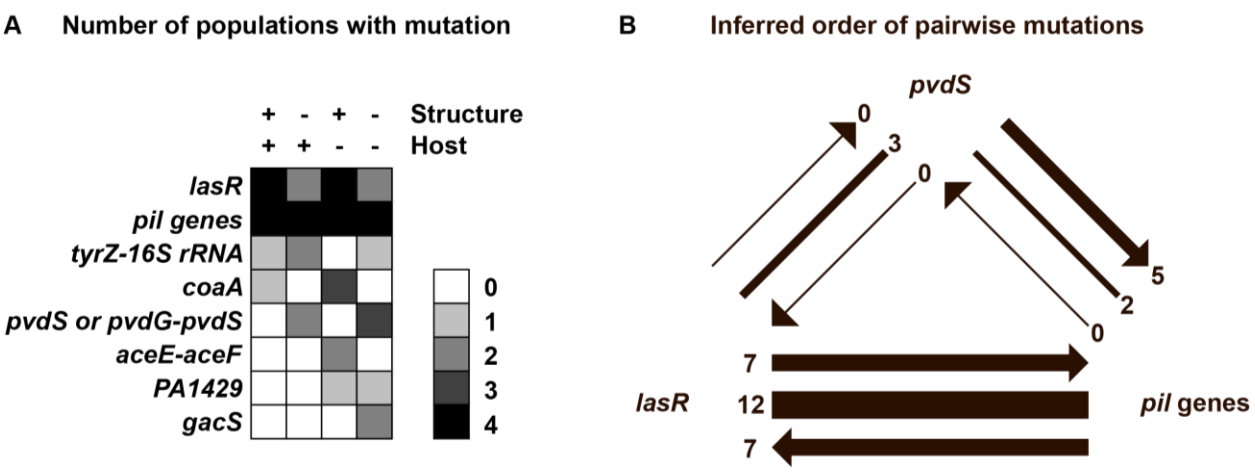

226

227 **Fig. 4. Whole genome sequencing reveals mutational profiles and order of mutations.** The whole
228 genomes of 140 evolved clones (four populations per environment and eight to nine clones per population)
229 were sequenced and SNPs and INDELs were called relative to the ancestral wildtype. **(A)** List of the loci
230 that were mutated in at least two populations. The scale of grey shadings corresponds to the number of
231 populations from each experimental condition in which clones with mutations in the respective loci
232 occurred. (**B**) Phylogenetic interference of the order of mutations among clones harboring mutations in two
233 of the most frequently concerned loci. Order of mutations are indicated by arrows pointing towards the loci
234 that were mutated second. Lines without arrowheads indicate that phylogenetic inference could not resolve
235 the order of mutations.

We found that two of these frequently mutated targets explained a large proportion of the altered virulence factor phenotypes (Fig. 5). Specifically, reduced pyoverdine production was significantly associated with mutations in the *pvdS* gene or its promoter region ($F(1,137) = 240.1$, $p < 0.0001$, Fig. 5A). Moreover, there were significant correlations between reduced pyocyanin and protease production and mutations in *lasR* (pyocyanin: $F(1,137) = 18.76$, $p < 0.0001$; proteases: $F(1,137) = 16.04$, $p < 0.001$, Fig. 5B+C). In roughly half of the clones (pyocyanin: 51.3%, proteases: 45.6%), reduced production levels could be attributed to mutations in *lasR*. While the Las-system directly controls the expression of proteases, pyocyanin is only indirectly linked to this QS-system, via the two subordinate Rhl and PQS quorum sensing systems [46]. We further analyzed whether the mutations in the type IV pili genes affected biofilm formation. Although type IV pili can be important for bacterial attachment to surfaces [47], there was no clear relationship between these mutations and the evolved biofilm phenotypes (Fig. S5). This is probably because biofilm formation is a quantitative trait, involving many genes, and because we found both evolution of increased and decreased biofilm production, which complicates the phenotype-genotype matching.

Mutational patterns reveal evidence for positive selection and parallel evolution

To test whether the mutated loci were under positive selection, we calculated the relative rates of nonsynonymous to synonymous SNPs (dN/dS) for loci mutated in at least two populations and for loci mutated only once. We found dN/dS = 6.2 for loci mutated in parallel in multiple populations, suggesting significant positive selection ($P(X \geq 74) \sim pois(\lambda=12) < 1.1 \times 10E\text{-}16$, where λ is the expected number of nonsynonymous SNPs under neutral evolution and X is the observed number of nonsynonymous SNPs). Conversely, dN/dS = 0.3 for loci mutated in only a single population,

indicating that these loci were under negative selection ($P(X \leq 26) \sim pois(\lambda=87) < 1.5 \times 10E\text{-}14$). Altogether, our findings reveal that the 18 loci with multiple mutations underwent adaptive parallel evolution.

Finally, we used phylogenetic inference to resolve the order of mutations involving the *lasR*, *pvdS*, and *pil* genes (Fig. 4B). Such analyses could reveal whether selection of mutations in certain genes is dependent on previous mutations in other genes. When analyzing evolved clones that mutated in at least two of these loci, we observed no clear patterns of dependencies in the order of mutations in *lasR*-*pil*-mutants and *lasR*-*pvdS*-mutants. For *pvdS*-*pil*-mutants, meanwhile, we found that mutations in *pvdS* tended to precede the mutations in *pil* genes. While sample size is too low to draw any strong conclusions, this observation could indicate that mutations in type IV pili are particularly beneficial in a pyoverdine-negative background.

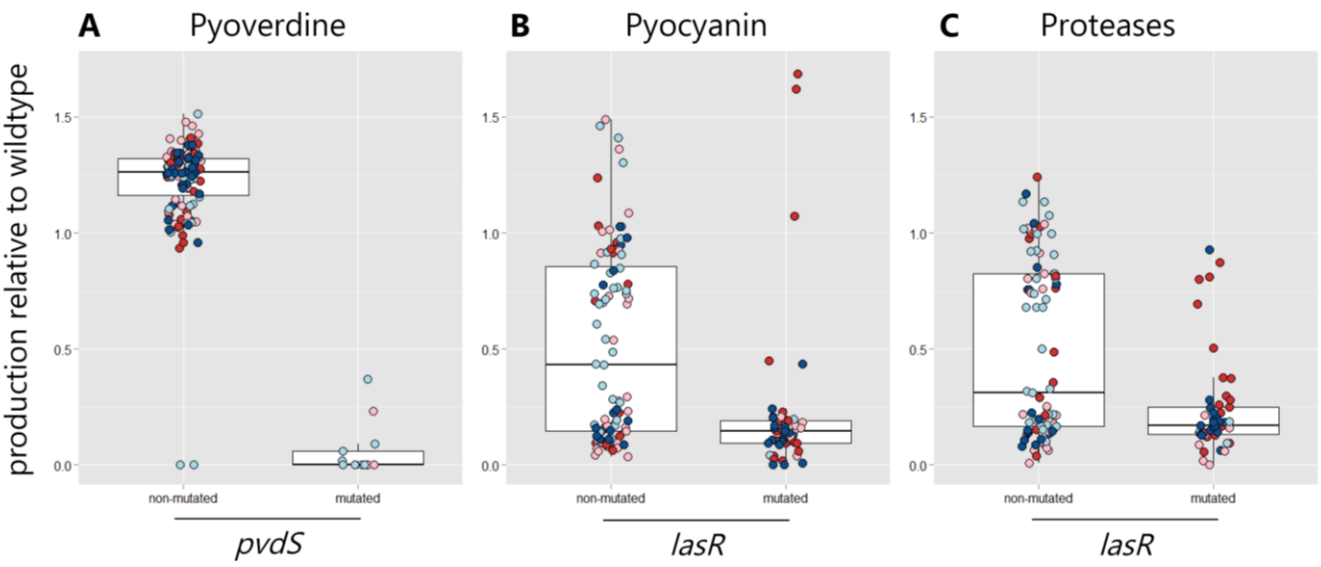

271

272 **Fig. 5. Mutations in key regulatory genes underlie the loss of virulence factor production.** Across the
273 140 successfully sequenced clones, there was an accumulation of mutations in two regulatory genes (*pvdS*
274 and *lasR*), which significantly correlated with the phenotypic changes observed for pyoverdine (**A**),
275 pyocyanin (**B**) and protease (**C**) production (see Table S2). *pvdS* encodes the iron starvation sigma factor
276 and all clones with mutations in this gene or its promoter showed significantly impaired pyoverdine
277 production. *lasR* encodes the regulator of the Las-quorum-sensing system, which directly controls the
278 expression of several proteases. All clones with *lasR* mutations showed reduced protease production. The
279 LasR regulator also has downstream effects on the Rhl- and PQS quorum-sensing systems, which control
280 pyocyanin production. Consistent with this view, most clones with *lasR* mutations (93.8 %) showed
281 decreased pyocyanin production. Although the genotype-phenotype match was nearly perfect for mutated
282 clones, a considerable amount of clones also showed altered phenotypes without mutations in these two
283 regulators, suggesting that some of the phenotypic changes are caused by mutations in yet unidentified loci.

DISCUSSION

Using the opportunistic human pathogen *P. aeruginosa*, we show that bacterial virulence can evolve rapidly during experimental evolution, as a result of adaptation to both the host and the non-host environment. Overall, we found that *P. aeruginosa* evolved greatly reduced virulence in liquid unstructured environments, but remained highly virulent in spatially structured environments, regardless of whether its nematode host was present or absent. Phenotypic and genotypic screens provide strong evidence for positive selection on bacterial virulence factors and parallel adaptive evolution across independent replicates. Virulence reduction in unstructured environments without hosts was driven by a sharp decline in the production of the siderophore pyoverdine, and moderate decreases in protease and pyocyanin production. Conversely, virulence reduction in unstructured environment with hosts is explained by a stark decrease in protease and pyocyanin production, but not pyoverdine. Although the traits under selection seem to vary as a function of host presence, our findings are in strong support of evolutionary theory predicting that low spatial structure should select for reduced pathogenicity if virulence is mediated by secreted compounds such as toxins, proteases or siderophores [5,9]. The reason for this is that secreted virulence factors can be shared between cells, and can thus become exploitable by cheating mutants that no longer contribute to costly virulence factor production, yet still capitalize on those produced by others. The spread of such mutants is predicted to reduce overall virulence factor availability and to curb virulence, exactly as observed in our study.

Our results highlight how an in-depth mechanistic analysis of the traits under selection can deepen our understanding of virulence evolution. In the absence of our phenotypic and genetic trait analysis, we would be tempted to conclude that the presence of the host has no effect on virulence

evolution, and that evolutionary change is entirely driven by the external non-host environment (Fig. 2). Our mechanistic trait analysis proves such conclusions wrong for multiple reasons. First, we observed strong selection for pyoverdine-negative mutants only in the absence but not in the presence of the host (Fig. 2A). Pervasive selection against pyoverdine in unstructured, yet iron-limited medium, has previously been attributed to cheating [14]. Here, we show that the spread of pyoverdine-cheaters is apparently prevented in the presence of the host. One reason for this host-specific effect might be that the spatial structure inside hosts counteracts the selective advantage cheaters experience outside the host. Second, we found that the presence of the host had a significant effect on the strength of selection against pyocyanin and protease production (Fig. 2B+C). We speculate that the presence of the host alters the reason for why these two virulence factors are selected against. In the absence of the host, neither pyocyanin nor proteases are required for growth, and their decline could be explained by selection against superfluous traits. Conversely, these two traits become beneficial in the presence of the host [38,40], such that selection against them could at least partially be explained by cheating. Third, we found evidence that the presence of the host selected for mutants with increased capacities to form biofilms (Fig. 2D). Apart from increasing residency time within hosts, the shift from a planktonic to a more sessile lifestyle typically goes along with fundamental changes in gene expression patterns [48,49], which might in turn affect virulence. Finally, we found that virulence factors were also under selection in treatments where the overall virulence level did not change (i.e. in structured environments). In these environments, however, reduced production of one virulence factor (e.g. protease and pyocyanin) was often compensated by the upregulation of other virulence factors (e.g. pyoverdine and biofilm), resulting in a zero net change in virulence.

A number of previous studies showed that when competition between virulence-factor producing and engineered non-producing bacteria is allowed for, then non-producing strains can often invade pathogen populations and thereby lower virulence [15,17,23,24]. While our work is in line with these findings, it makes several important novel contributions. First, our experiment started with fully virulent clonal wildtype bacteria, and any virulence-factor deficient mutants had to evolve from random mutations and invade pathogen populations from extreme rarity. Hence, our study proves that the predicted mutants indeed arise *de novo* and are promoted by natural selection in independent parallel replicates. Second, our results highlight that multiple social traits are simultaneously under selection, which contrasts with the work with engineered mutants, where either a specific siderophore or quorum-sensing system was deleted [15,17,23,24]. The fact that multiple differentially regulated virulence traits are under selection allowed us to identify additive and compensatory effects between traits, and to track the order of mutations. Third, our study design captured the cycling of an opportunistic pathogen through the host and the non-host environment, as it would occur under natural conditions [26,27]. This approach allowed us to discover accidental virulence effects that are purely driven by adaptation to the non-host environment. These non-host effects could not be quantified in previous studies, as the pathogens were directly transferred from one host generation to the next [17,23,24,50,51].

At the genetic level, our findings closely relate to previous work that has identified *lasR* as a key target of evolution in the context of chronic *P. aeruginosa* infections in the cystic fibrosis lung [52–56], in non-cystic fibrosis bronchiectasis [57], as well as in acute infections [18,51]. While the ubiquitous appearance of *lasR*-mutants was often interpreted as a specific host adaptation, we show here that *lasR*-mutants frequently arise even in the absence of a host, indicating that

353 mutations in *lasR* are not a host-specific phenomenon. We propose three mutually non-exclusive
354 explanations for the frequent occurrence and selective spread of *lasR*-mutants. First, we propose
355 that the Las-quorum-sensing regulon might no longer be beneficial under many of the culturing
356 conditions used in the laboratory, especially when bacteria are consistently grown at high cell
357 densities. Mutations in *lasR* would thus reflect the first step in the degradation of this system.
358 Alternatively, it is conceivable that quorum sensing remains beneficial, but that mutations in *lasR*
359 represent the first step in the rewiring of the QS network in order to customize it to the novel
360 conditions experienced in infections and laboratory cultures [58]. Finally, the invasion of *lasR*-
361 mutants could be the result of cheating, where these signal blind mutants still contribute to signal
362 production, but no longer respond to it and thus refrain from producing the QS-controlled public
363 goods [36,59]. We have argued above that, although *lasR* mutants were favoured in all our
364 treatments, the presence of the host might change the selection pressure and underlying reason for
365 why these mutants are selected for. More generally, our observations of high strain diversification
366 during experimental evolution, and the co-existence of multiple different phenotypes and
367 genotypes within each replicate, are reminiscent of patterns found in chronic *P. aeruginosa*
368 infections in cystic fibrosis lungs [19,52,53,60]. While this diversity might be transient in some
369 cases, it highlights that an initially clonal infection can give rise to a diverse community, with
370 multiple strains competing with each other within the host, as it was observed in CF lung
371 communities [61,62].
372
373 In conclusion, our study demonstrates that there is rapid and parallel virulence evolution in
374 populations of the opportunist *P. aeruginosa*, and that secreted virulence factors are the main target
375 of selection. While low spatial structure of the environment generally selected for lower virulence

regardless of whether hosts were present or not, the virulence traits under selection and the strength of selection were host dependent. This greatly contributes to our knowledge on how bacterial opportunistic pathogens adapt to the variable environments they occupy, and how this affects their virulence [26,27]. Our work also highlights that linking virulence evolution to selection inside and outside of the host is key to predict evolutionary trajectories in opportunistic pathogens. Such insights might offer simple approaches of how to manage infections in these clinically highly important pathogens [60,63–65], for example through the disruption of spatial structure in chronic infections, which could, according to our findings, steer pathogen evolution towards lower virulence.

MATERIALS AND METHODS

Strains and growth conditions

We used *Pseudomonas aeruginosa* wildtype strain PAO1 (ATCC 15692) constitutively expressing GFP (PAO1-*gfp*) for experimental evolution. The siderophore deficient mutant PAO1Δ*pvdD-gfp*, the quorum-sensing deficient mutants PAO1Δ*rhlR* and PAO1Δ*lasR* (S. Diggle, Georgia Institute of Technology, USA), and the biofilm deficient mutant MPAO1Δ*pelA*Δ*pslA* (M. Toyofuku, University of Zurich, Switzerland) were used as negative controls for phenotype screening. For overnight pre-culturing, we routinely used Luria Bertani (LB) medium and incubated the bacteria under shaking conditions (190 rpm) for 18-20 h, and optical density (OD) of bacterial cultures was determined in a Tecan Infinite M-200 plate reader (Tecan Group Ltd., Switzerland) at a wavelength of 600 nm, unless indicated otherwise. All experiments in this study were conducted at 25°C, except for the pre-culturing of the ancestral wildtype strain before the start of the experimental evolution (see below). To generate iron-limited nutrient medium (RDM-Ch) suitable for bacterial and nematode co-culturing, we supplied low-phosphate NGM (nematode growth medium; 2.5 gL^{-1} BactoPeptone, 3 gL^{-1} NaCl, 5 mgL^{-1} Cholesterol, 25 mM MES buffer pH = 6.0, 1mM MgSO4, 1mM $CaCl_2$; adapted from [30] with the iron chelator 2,2'-Bipyridyl at a final concentration of 200 µM. For agar plates, liquid media was supplemented with 1.5% (m/V) agar. All chemicals were acquired from Sigma-Aldrich, Switzerland. *Caenorhabditis elegans* N2 wildtype nematodes were acquired from the Caenorhabditis Genetics Center (CGC). General nematode maintenance and generation of age-synchronized L4 nematodes was performed according to standard protocols [66].

406 **Experimental evolution**

407 Experimental evolution was conducted with a clonal population of PAO1-*gfp* bacteria as a starting
408 point. For each of the four experimental treatments (agar plates with and without host, liquid
409 culture with and without host), eight replicate lines were evolved independently. Throughout the
410 experimental evolution, *C. elegans* was not allowed to co-evolve. Instead, fresh age-synchronized
411 L4 stage nematodes were supplied at each transfer step. Since *P. aeruginosa* is highly virulent
412 towards *C. elegans*, the vast majority of worms were dead before each transfer step. Each
413 individual culture was visually checked for egg or L1 larvae development and we never observed
414 any live larvae. We can therefore assume that the nematodes did not successfully reproduce during
415 experimental evolution.

416

417 At the start of the experimental evolution, overnight cultures of PAO1-*gfp* were grown under
418 shaken conditions (190-200 rpm) at 37°C for 18 h, washed with NaCl (0.85%) and adjusted to an
419 OD600 of 1.0. After this point, all steps throughout the experimental evolution were conducted at
420 25°C. For evolution on agar plates and for each replicate line, 50 µL of cell suspension were spread
421 onto a small RDM-Ch agar plate (diameter 60 mm). Approximately 100 age-synchronized L4
422 stage *C. elegans* nematodes were then added to each plate in the treatment "agar plate with host",
423 and all plates were incubated for 48 h before the first transfer. For evolution in liquid cultures, the
424 same OD-adjusted bacterial suspensions were diluted 10^{-4} into 5 mL of liquid RDM-Ch in 15 mL
425 culture tubes. Approximately 2500 age-synchronized L4 stage *C. elegans* nematodes were then
426 added to each tube for the treatment "liquid culture with host", and all tubes were incubated for
427 48 h under "rolling" conditions (160 rpm) in a horizontal position to avoid clumping of the worms.
428 Transfers of bacteria to fresh nutrient medium and, if applicable, addition of fresh nematodes to

the samples were conducted every 48 h and executed as follows. For all agar plates, bacteria were replica-plated to a fresh RDM-Ch plate, using a custom made replica tool covered in sterilized velvet. In the treatment "agar plate with host", the plates containing the nematodes from the previous round were then rinsed off the plate with sterile NaCl (0.85%), washed thoroughly to avoid additional transfer of bacteria, and 10% of the nematode suspension was transferred to the new plate. Since *P. aeruginosa* is highly virulent towards *C. elegans*, the transferred worms were carcasses. A fresh batch of ~100 synchronized L4 stage nematodes was then added to the plates. For the "liquid culture without host" treatment, 50 µL of the culture was used to inoculate 4.95 mL of fresh RDM-Ch medium. For the "liquid culture with host" treatment, culture tubes were centrifuged slowly (~200 g, 5 min) to pellet the nematodes, and 50 µL of the supernatant (still containing the bacteria) was used to inoculate 4.95 mL of fresh RDM-Ch medium. The pelleted nematodes were then washed thoroughly with sterile NaCl (0.85%), and 10% of the nematode suspension was transferred to the new culture tube. Analogous to the agar treatment, most transferred worms were carcasses due to the high virulence levels of *P. aeruginosa*. A fresh batch of ~2500 synchronized L4 nematodes was then added to the tubes.

The number of viable bacteria transferred through replica-plating corresponded approximately to a 1:100 dilution, and was therefore equivalent to the dilution achieved in the liquid cultures. In total, 30 transfers were conducted, corresponding to approximately 200 generations of bacterial evolution. At the end of the experimental evolution, evolved populations were frozen for further analysis as follows. For the two agar plates treatments, the bacterial lawn was washed off with sterile NaCl (0.85%), mixed vigorously, diluted 10^{-3} into 3 mL of liquid LB medium in 6-well plates, and incubated under shaken conditions (100 rpm) for 18 h. For the "liquid culture with

host" treatment, culture tubes were first centrifuged slowly (~200 g, 5 min) to pellet the nematodes. Then, 25 µL of the supernatant (containing bacteria) was used to inoculate 2.475 mL liquid LB medium in 6-well plates. For the "liquid culture without host" treatment, 25 µL of the bacterial culture was used to inoculate 2.475 mL liquid LB medium in 6-well plates. All plates were then incubated under shaken conditions (100 rpm) for 18 h. Finally, 900 µL of each well was mixed 1:1 with sterile glycerol (85%) and frozen at -80°C in separate cryotubes.

Killing assays for virulence measurements

Population level virulence was assessed in two different killing assays, namely in liquid culture and on agar plates, representing the two different environments the different bacterial populations evolved in. Populations were separately tested both in the environment they evolved in (populations evolved on agar plates tested on agar plates, and populations evolved in liquid culture tested in liquid culture), and in the respective reciprocal environment (populations evolved in liquid culture tested on agar plates, and vice versa). All killing assays were conducted at 25°C.

For killing assays in liquid culture, evolved bacterial populations and the ancestral wildtype strain were re-grown from freezer stocks in LB medium overnight, washed with sterile NaCl (0.85%), adjusted to OD600=1.0 and diluted 10^{-4} into 5 mL of liquid RDM-Ch medium in a 15 mL culture tube. Three replicate tubes were inoculated per tested population. After an incubation period of 48 h (shaken conditions, 160-165 rpm), the OD600 was measured and cells were pelleted through centrifugation. A volume ≤ 500 µL of the supernatant was removed, corresponding to the volume containing ~2500 synchronized L4 nematodes that were subsequently added. Culture tubes were

475 then incubated for 48 h under "rolling" conditions at 160 rpm in a horizontal position to avoid
476 clumping of the worms. At 24 h and 48 h after adding the nematodes, the level of virulence was
477 determined by counting the fraction of dead worms. Small aliquots were taken from the main
478 culture and dropped onto an NGM plate. After a short drying period, nematodes were prodded
479 repeatedly with a metal rod and counted as dead if they did not show any signs of movement. Dead
480 worms were immediately removed to avoid double counting.
481
482 For killing assays on agar plates, evolved bacterial populations and the ancestral wildtype strain
483 were re-grown from freezer stock in LB medium overnight, washed with sterile NaCl (0.85%),
484 adjusted to OD600=1.0 and 50 µL were spread on RDM-Ch agar plates. Six replicate plates were
485 inoculated per tested population. Plates were incubated for 48 h, and an aliquot of synchronized
486 L4 nematodes suspended in liquid was then added to the plates. The nematodes had been
487 previously starved on empty NGM plates for 24 h. The starting number of nematodes ranged from
488 20 to 60 worms per plate and was immediately determined by manual counting. Plates were then
489 incubated further and at 24 h and 48 h after adding the nematodes, the level of virulence was
490 determined by counting the number of dead worms on the plates, as described for the killing assay
491 in liquid culture. For both killing assays, each individual liquid culture and plate was visually
492 checked for egg or L1 larvae development and we never observed any live larvae. We can therefore
493 assume that the nematodes did not successfully reproduce during these experiments.
494
495 **Isolation of single clones**
496 To isolate single clones, evolved bacterial populations were re-grown from freezer stock in 3 mL
497 LB medium for 20 h (160 rpm) and adjusted to OD600=1.0. Then, 200 µL of 10^{-6} and 10^{-7} dilutions

were spread on large LB agar plates (diameter 150 mm), and plates were incubated at room temperature (~20-25°C) for 48 h. Twenty colonies were then randomly picked for each population and inoculated into 100 µL LB medium in a 96-well plate. Plates were incubated for 24 h under shaken conditions (165 rpm) before adding 100 µL sterile glycerol (85%) to each well, sealing the plates with adhesive foil and freezing at -80°C. A total number of 640 clones was isolated this way, and each was subjected to four different phenotypic screens for virulence factor production.

Phenotypic screen for virulence factor production

Pyoverdine production. Single clones were re-grown from freezer stocks in 200 µL LB medium for 20 h (165 rpm) in 96-well plates. Then, for each well, cultures were first diluted 10^{-2} in NaCl (0.85%) and then 10^{-2} into liquid RDM-Ch to a final volume of 200 µL in a 96-well plate. Plates were then incubated for 24 h under shaken conditions (165 rpm) and OD600 and pyoverdine-specific fluorescence (emission 400 nm, excitation 460 nm) were measured in a plate reader through single endpoint measurements. Multiple wells inoculated with the ancestral wildtype as well as blank medium controls were included in every plate. Additionally, the pyoverdine knockout mutant PAO1-Δ*pvdD-gfp* was included as a negative control for pyoverdine fluorescence.

Pyocyanin production. Single clones were re-grown from freezer stocks in 200 µL LB medium for 20 h (165 rpm) in 96-well plates. Then, for each well, cultures were first diluted 10^{-2} in NaCl (0.85%) and then 10^{-2} into liquid LB to a final volume of 1 mL in 24-well plates. Plates were then incubated for 24 h under shaken conditions (165 rpm). The well content was then transferred to 1.5 mL reaction tubes, vortexed thoroughly, and centrifuged to pellet bacterial cells. From each

tube, three aliquots of 150 µL of the cell-free supernatant were then transferred to 96-well plates, and pyocyanin was quantified by measuring OD at 691 nm in a plate reader. Multiple wells inoculated with the ancestral wildtype as well as blank medium controls were included in every plate. Additionally, the Rhl-quorum-sensing deficient knockout mutant PAO1-Δ*rhlR* was included as a negative control for pyocyanin production.

Protease production. Single clones were re-grown from freezer stocks in 200 µL LB medium for 20 h (165 rpm) in 96-well plates. Then, for each well, 1 µL of bacterial culture was dropped into a single well of a 24-well plate filled with skim milk agar (5 gL^{-1} LB, 4% (m/V) skim milk powder, 15 gL^{-1} agar) and plates were incubated for 20 h. Pictures of the plates were then taken with a standard digital camera and analyzed with the Image Analysis Software *ImageJ* [67]. The diameter of the clear halo around the bacterial colony and the diameter of the colony itself was measured, and protease production was calculated using the following formula:

$$relative\ protease\ production = \frac{(diameter(halo) - diameter(colony))}{diameter(colony)}.$$

Multiple wells inoculated with the ancestral wildtype as well as blank medium controls were included in every plate. Additionally, the Las-quorum-sensing deficient knockout mutant PAO1-Δ*lasR* was included as a negative control for protease production.

Biofilm production. Single clones were re-grown from freezer stocks in 200 µL LB medium for 20 h (165 rpm) in 96-well plates. Then, for each well, the air liquid biofilm was manually removed from the surface with a sterile pipette tip. Cultures were then diluted 10^{-2} into 100 µL LB medium in a 96-well round bottom plate (No. 83.3925.500, Sarstedt, Germany) and incubated under static conditions for 24 h. After removal of the air liquid biofilm, the growth medium containing the

544 planktonic cells was transferred to a fresh flat-bottom 96-well plate and OD was measured at
545 550 nm in a plate reader. In the plate containing the cells attached to the plastic surface, 100 µL of
546 crystal violet (0.1%) was added to each well and plates were incubated at room temperature for
547 30 min. Then, the wells were carefully washed several times with ddH_2O, left to dry at room
548 temperature for 30 min, and 120 µL DMSO was added to each well before a final incubation step
549 of 20 min at room temperature. Finally, OD was measured at 570 nm in a plate reader, and the
550 production of surface-attached biofilms was quantified by calculating the "Biofilm Index"
551 (OD570/OD550) for each well [68]. Multiple wells inoculated with the ancestral wildtype as well
552 as blank medium controls were included in every plate. Additionally, the knockout mutant
553 MPAO1-Δ*pelA*-Δ*pslA* was included as a negative control for biofilm production.
554
555 **Calculation of the "virulence factor index".** We defined a virulence factor index $v = \Sigma\, r_i / n$,
556 where r_i-values represent the average virulence factor production scaled relative to the ancestral
557 wildtype for the *i*-th virulence factor (*i* = pyoverdine, pyocyanin, proteases, biofilm), and *n* is the
558 total number of virulence factors. A clone with wildtype production levels for all four virulence
559 factors measured would have a virulence index of ~1, whereas a clone with mostly lowered or
560 absent production would have a virulence index closer to 0. For statistical analyses and the
561 generation of Fig. 3B and Fig. S3, we used the average virulence index across clones for each
562 population.

563 **Whole genome sequencing and variant calling**

564

565 **Selection of clones to sequence.** To select populations from which to select clones for sequencing,
566 we first chose all populations that showed a decrease in virulence, and then added randomly chosen
567 populations to cover all four treatments in a balanced way (four sequenced populations for each
568 treatment), leading to a total of 16 selected evolved populations. From these, we selected 9 clones
569 per population according to the following scheme: first, we tried to get at least one clone that
570 showed no phenotypic differences to the ancestral wildtype with regards to pyoverdine and
571 pyocyanin production. Then, we tried to get clones with a marked decrease in pyoverdine and/or
572 pyocyanin production. Finally, we filled up the list with randomly chosen clones.

573

574 **Genomic DNA isolation.** Clones were re-grown from freezer stocks in 3 mL LB medium in 15 mL
575 culture tubes at 190 rpm for 20-24 h. Genomic DNA was then extracted from 1 mL of culture
576 using the *GenElute™ Bacterial Genomic DNA Kit* (Sigma-Aldrich, Switzerland) according to the
577 manufacturer's instructions. At the final step of the isolation protocol, the DNA was eluted in
578 TRIS-HCl without the addition of EDTA to avoid interference with sequencing library preparation.
579 DNA concentration was quantified using the *QuantiFluor® dsDNA System* (Promega,
580 Switzerland) according to the manufacturer's instructions, and diluted to a concentration of
581 10 ng/µL for use in subsequent library preparation.

582

583 **Preparation of sequencing library and whole genome sequencing.** Sequencing libraries were
584 constructed using the Nextera XT Kit (Illumina, USA). Briefly, 0.8 ng of gDNA per sample was
585 tagmented at 55 °C for 10 min. Libraries were dual-indexed and amplified in the subsequent library

PCR. Sequencing libraries were cleaned up using cleanNA SPRI beads (GC biotech, Netherlands) according to the manufacturer's protocol. Next, DNA concentration was quantified using the *QuantiFluor® dsDNA System* (Promega, Germany) and equal amounts of library per sample pooled. Finally, the molarity of the library pool was determined using the *dsDNA High Sensitivity Assay* for the *Bioanalyzer 2100* (Agilent Technologies, Germany). Sequencing was performed 2x150 bp by Microsynth (Balgach, Switzerland) on a NextSeq500 (Illumina, USA).

Variant calling. Demultiplexed reads were aligned to the *P. aeruginosa* PAO1 reference genome using bowtie2 in local-sensitive mode [69]. PCR duplicates were removed using "picard" tools (https://broadinstitute.github.io/picard/). Variants were called using "samtools" (v0.1.19), "mpileup" and "bcftools" [70]. Variants were filtered with default parameters using "samtools" and "vcfutils". Variant effects were predicted using SnpEff (version 4.1d) [71]. Annotated variant calls were only retained if more than 80% of reads contained the alternate base and if quality scores (Phred-scaled probability of sample reads being homozygous reference) were at least 50 (i.e. $P \leq$ 10E-5). All variants already occurring in the ancestral wildtype strain were discarded for analysis of the evolved clones. Of the 144 sequenced clones, three had to be discarded before analysis due to low coverage, and one for likely being a mixture of two different genotypes due to contamination. Read alignments covering genes with multiple variants (either in the same or different clones) were manually inspected to remove spurious calls in 19 loci (PA2139-PA2140, PA4875-PA4876, PA3503-PA3504, PA2127-PA2128, PA0604-PA0605, PA0366-PA0367, PA0148-PA0149, PA5024, PA4526-PA4527, PA3969a-PA3970, PA1352-PA1353, PA4280.2-PA4280.3, PA2000-PA2001, PA1234-PA1235, PA4838-PA4839, PA2373, PA2232, PA2296, and PA2492).

609 **Analysis of parallelism and order of mutations.**

610 We based our calculation of the relative rates of nonsynonymous to synonymous SNPs (dN/dS)
611 on a 25% chance that a random substitution mutation would be synonymous. In the case of the
612 *P. aeruginosa* genomes we analyzed here, out of a total of 16,779,042 possible SNP mutations
613 within the genes (5,593,014 bp of coding sequences, multiplied by three possible mutations in each
614 position), only 4,237,247 SNP mutations would cause a synonymous change.
615 To infer the order of mutations, we compared the mutations that were called across strains from
616 the 16 populations, and identified 18 loci (i.e. genes or an intergenic regions) that were mutated in
617 at least two populations. The Supplementary Table S3 lists all mutations in the 18 loci that were
618 mutated in at least two populations, and also lists mutations in *pilE pilG*, *pilM*, *pilN*, *pilO*, *pilU*,
619 *pilW*, and *pilZ* that were only mutated in a single population. To order two given mutations in a
620 given strain, we checked whether other strains from the same population carried only one of these
621 two mutations, as this would indicate that the other mutation appeared second in the same strain.
622 We observed no mutational patterns inconsistent with this model.
623

624 **Statistical Analysis**

625 We used linear models and linear mixed models for statistical analyses using R 3.2.2 [72]. In cases
626 where data distributions did not meet the assumptions of linear models, we performed non-
627 parametric Wilcoxon rank sum tests. To test whether evolved virulence factor production in single
628 clones depended on the environment they evolved in, we used Markov-chain Monte Carlo
629 generalized linear mixed models (MCMCglmm) in a Bayesian framework [73]. In this context, *p*
630 represents the posterior probability associated with a fixed effect, and as such is not a “classical”
631 frequentist p-value, but provides the same kind of information. For all results analyzed with

632 MCMCglmm, we ran the analyses at least five consecutive times to confirm that p-values were
633 consistently < 0.05. Principal component analysis (PCA) was conducted using the 'FactoMineR'
634 [74] and 'factoextra' packages (https://CRAN.R-project.org/package=factoextra). Detailed
635 information on the results of all statistical tests associated with this publication can be found in
636 Supplementary Table S2.

ACKNOWLEDGEMENTS

We thank Swati Parekh for assistance in genomic analysis, Isa Moreno for help with the nematode killing assays, Ruben Dezeure for statistical advice, and Stu West and Sam Brown for comments on the manuscript.

AUTHOR CONTRIBUTIONS

E.G. and R.K. planned the experiments. E.G. carried out the experiments and conducted statistical analysis. C.Z. constructed the sequencing libraries and carried out variant calling. R.L.M. analysed the variants. E.G. and R.K. analyzed and interpreted the data. All authors contributed to writing the manuscript.

FUNDING DISCLOSURE

This work was funded by the Swiss National Science Foundation (grant no. PP00P3_165835), the ERC (grant no. 681295), and the Forschungskredit of the University of Zurich (no. FK-15-084). RLM is supported by the Danish National Research Foundation (grant no. 126). *C. elegans* strains were provided by the CGC, which is funded by NIH Office of Research Infrastructure Programs (P40 OD010440).

DATA AVAILABILITY

All sequencing data is available at the European Nucleotide Archive (accession number PRJEB23190). We will deposit all raw data on Dryad and will provide all respective accession numbers at the revision stage.

REFERENCES

1. Cressler CE, McLeod D V., Rozins C, Van den Hoogen J, Day T. The adaptive evolution of virulence: a review of theoretical predictions and empirical tests. Parasitology. 2016; 915–930.
2. Diard M, Hardt W-D. Evolution of bacterial virulence. FEMS Microbiol Rev. 2017; 679–697.
3. Frank SA. Models of Parasite Virulence. Q Rev Biol. 1996; 37–78.
4. Wild G, Gardner A, West SA. Adaptation and the evolution of parasite virulence in a connected world. Nature. 2009; 983–6.
5. Buckling A, Brockhurst MA. Kin selection and the evolution of virulence. Heredity. 2008; 484–8.
6. Lion S. Multiple infections, kin selection and the evolutionary epidemiology of parasite traits. J Evol Biol. 2013; 2107–2122.
7. Alizon S, de Roode JC, Michalakis Y. Multiple infections and the evolution of virulence. Ecol Lett. 2013; 556–567.
8. de Roode JC, Pansini R, Cheesman SJ, Helinski MEH, Huijben S, Wargo AR, et al. Virulence and competitive ability in genetically diverse malaria infections. Proc Natl Acad Sci U S A. 2005; 7624–8.
9. West SA, Buckling A. Cooperation, virulence and siderophore production in bacterial parasites. Proc Biol Sci. 2003; 37–44.
10. Alizon S, Lion S. Within-host parasite cooperation and the evolution of virulence. Proc Biol Sci. 2011; 3738–3747.
11. West SA, Diggle SP, Buckling A, Gardner A, Griffin AS. The Social Lives of Microbes. Annu Rev Ecol Evol Syst. 2007; 53–77.
12. Brown SP, Hochberg ME, Grenfell BT. Does multiple infection select for raised virulence? Trends Microbiol. 2002; 401–5.
13. Buckling A, Harrison F, Vos M, Brockhurst MA, Gardner A, West SA, et al. Siderophore-mediated cooperation and virulence in Pseudomonas aeruginosa. FEMS Microbiol Ecol. 2007; 135–141.
14. Kümmerli R, Griffin AS, West SA, Buckling A, Harrison F. Viscous medium promotes cooperation in the pathogenic bacterium Pseudomonas aeruginosa. Proc Biol Sci. 2009;

690 3531–8.
691 15. Harrison F, Browning LE, Vos M, Buckling A. Cooperation and virulence in acute
692 Pseudomonas aeruginosa infections. BMC Biol. 2006; 21.
693 16. Raymond B, West SA, Griffin AS, Bonsall MB. The dynamics of cooperative bacterial
694 virulence in the field. Science. 2012; 85–8.
695 17. Rumbaugh KP, Diggle SP, Watters CM, Ross-Gillespie A, Griffin AS, West SA. Quorum
696 Sensing and the Social Evolution of Bacterial Virulence. Curr Biol. 2009; 341–345.
697 18. Köhler T, Buckling A, van Delden C. Cooperation and virulence of clinical Pseudomonas
698 aeruginosa populations. Proc Natl Acad Sci U S A. 2009; 6339–44.
699 19. Andersen SB, Marvig RL, Molin S, Krogh Johansen H, Griffin AS. Long-term social
700 dynamics drive loss of function in pathogenic bacteria. Proc Natl Acad Sci. 2015; 10756–
701 10761.
702 20. Boots M, Mealor M. Local interactions select for lower pathogen infectivity. Science. 2007;
703 1284–6.
704 21. Kerr B, Neuhauser C, Bohannan BJM, Dean AM. Local migration promotes competitive
705 restraint in a host-pathogen "tragedy of the commons". Nature. 2006; 75–8.
706 22. Leggett HC, Wild G, West SA, Buckling A, Leggett HC. Fast-killing parasites can be
707 favoured in spatially structured populations. Philos Trans R Soc Lond B Biol Sci. 2017; 1–
708 5.
709 23. Rumbaugh KP, Trivedi U, Watters C, Burton-Chellew MN, Diggle SP, West SA. Kin
710 selection, quorum sensing and virulence in pathogenic bacteria. Proc Biol Sci. 2012; 3584–
711 3588.
712 24. Pollitt EJG, West SA, Crusz S a, Burton-Chellew MN, Diggle SP. Cooperation, Quorum
713 Sensing, and Evolution of Virulence in Staphylococcus aureus. Infect Immun. 2014; 1045–
714 51.
715 25. Leggett HC, Cornwallis CK, Buckling A, West SA. Growth rate, transmission mode and
716 virulence in human pathogens. Philos Trans R Soc B Biol Sci. 2017; 20160094.
717 26. Brown SP, Cornforth DM, Mideo N. Evolution of virulence in opportunistic pathogens:
718 generalism, plasticity, and control. Trends Microbiol. 2012; 336–42.
719 27. Brown NF, Wickham ME, Coombes BK, Finlay BB. Crossing the line: Selection and
720 evolution of virulence traits. PLoS Pathog. 2006; 346–353.

721 28. Mikonranta L, Mappes J, Laakso J, Ketola T. Within-host evolution decreases virulence in
722 an opportunistic bacterial pathogen. BMC Evol Biol. 2015; 165.
723 29. Tan MW, Mahajan-Miklos S, Ausubel FM. Killing of Caenorhabditis elegans by
724 Pseudomonas aeruginosa used to model mammalian bacterial pathogenesis. Proc Natl Acad
725 Sci U S A. 1999; 715–20.
726 30. Zaborin A, Romanowski K, Gerdes S, Holbrook C, Lepine F, Long J, et al. Red death in
727 Caenorhabditis elegans caused by Pseudomonas aeruginosa PAO1. Proc Natl Acad Sci U S
728 A. 2009; 6327–32.
729 31. de Abreu P, Farias P, Paiva G, Almeida A, Morais P. Persistence of microbial communities
730 including Pseudomonas aeruginosa in a hospital environment: a potential health hazard.
731 BMC Microbiol. 2014; 118.
732 32. Green S, Schroth M, Cho J. Agricultural plants and soil as a reservoir for Pseudomonas
733 aeruginosa. Appl Microbiol. 1974; 987–991.
734 33. Samuel BS, Rowedder H, Braendle C, Félix M-A, Ruvkun G. Caenorhabditis elegans
735 responses to bacteria from its natural habitats. Proc Natl Acad Sci. 2016; E3941–E3949.
736 34. Schalk IJ, Guillon L. Pyoverdine biosynthesis and secretion in Pseudomonas aeruginosa:
737 implications for metal homeostasis. Environ Microbiol. 2013; 1661–73.
738 35. Lau GW, Hassett DJ, Ran H, Kong F. The role of pyocyanin in Pseudomonas aeruginosa
739 infection. Trends Mol Med. 2004; 599–606.
740 36. Diggle SP, Griffin AS, Campbell GS, West SA. Cooperation and conflict in quorum-sensing
741 bacterial populations. Nature. 2007; 411–414.
742 37. van Tilburg Bernardes E, Charron-Mazenod L, Reading DJ, Reckseidler-Zenteno SL,
743 Lewenza S. Exopolysaccharide-repressing small molecules with antibiofilm and
744 antivirulence activity against Pseudomonas aeruginosa. Antimicrob Agents Chemother.
745 2017; AAC.01997-16.
746 38. Cezairliyan B, Vinayavekhin N, Grenfell-Lee D, Yuen GJ, Saghatelian A, Ausubel FM.
747 Identification of Pseudomonas aeruginosa phenazines that kill Caenorhabditis elegans.
748 PLoS Pathog. 2013.
749 39. Van Tilburg Bernardes E, Charron-Mazenod L, Reading DJ, Reckseidler-Zenteno SL,
750 Lewenza S. Exopolysaccharide-repressing small molecules with antibiofilm and
751 antivirulence activity against Pseudomonas aeruginosa. Antimicrob Agents Chemother.

2017; AAC.01997-16.

40. Zhu J, Cai X, Harris TL, Gooyit M, Wood M, Lardy M, et al. Disarming Pseudomonas aeruginosa Virulence Factor LasB by Leveraging a Caenorhabditis elegans Infection Model. Chem Biol. 2015; 483–491.

41. Dumas Z, Kümmerli R. Cost of cooperation rules selection for cheats in bacterial metapopulations. J Evol Biol. 2012; 473–484.

42. Kümmerli R, Santorelli LA, Granato ET, Dumas Z, Dobay A, Griffin AS, et al. Co-evolutionary dynamics between public good producers and cheats in the bacterium Pseudomonas aeruginosa. J Evol Biol. 2015; 2264–74.

43. Ross-Gillespie A, Weigert M, Brown SP, Kümmerli R. Gallium-mediated siderophore quenching as an evolutionarily robust antibacterial treatment. Evol Med Public Heal. 2014; 18–29.

44. Bonchi C, Frangipani E, Imperi F, Visca P. Pyoverdine and proteases affect the response of pseudomonas aeruginosa to gallium in human serum. Antimicrob Agents Chemother. 2015; 5641–5646.

45. Lim WS, Phang KKS, Tan AHM, Li SFY, Ow DSW. Small colony variants and single nucleotide variations in Pf1 region of Pb1 phage-resistant Pseudomonas aeruginosa. Front Microbiol. 2016; 1–14.

46. Lee J, Zhang L. The hierarchy quorum sensing network in Pseudomonas aeruginosa. Protein Cell. 2014; 26–41.

47. Barken KB, Pamp SJ, Yang L, Gjermansen M, Bertrand JJ, Klausen M, et al. Roles of type IV pili, flagellum-mediated motility and extracellular DNA in the formation of mature multicellular structures in Pseudomonas aeruginosa biofilms. Environ Microbiol. 2008; 2331–2343.

48. Sauer K, Camper AK, Ehrlich GD, Costerton JW, Davies DG. Pseudomonas aeruginosa. J Bacteriol. 2002; 1140–1154.

49. Rollet C, Gal L, Guzzo J. Biofilm-detached cells, a transition from a sessile to a planktonic phenotype: A comparative study of adhesion and physiological characteristics in pseudomonas aeruginosa. FEMS Microbiol Lett. 2009; 135–142.

50. Racey D, Inglis RF, Harrison F, Oliver A, Buckling A. The effect of elevated mutation rates on the evolution of cooperation and virulence of Pseudomonas aeruginosa. Evolution. 2010;

515–21.

51. Jansen G, Crummenerl LL, Gilbert F, Mohr T, Pfefferkorn R, Thänert R, et al. Evolutionary transition from pathogenicity to commensalism: Global regulator mutations mediate fitness gains through virulence attenuation. Mol Biol Evol. 2015; 2883–2896.
52. Marvig RL, Sommer LM, Molin S, Johansen HK. Convergent evolution and adaptation of Pseudomonas aeruginosa within patients with cystic fibrosis. Nat Genet. 2015; 57–65.
53. Winstanley C, O'Brien S, Brockhurst MA. Pseudomonas aeruginosa Evolutionary Adaptation and Diversification in Cystic Fibrosis Chronic Lung Infections. Trends Microbiol. 2016; 327–337.
54. Hoffman LR, Kulasekara HD, Emerson J, Houston LS, Burns JL, Ramsey BW, et al. Pseudomonas aeruginosa lasR mutants are associated with cystic fibrosis lung disease progression. J Cyst Fibros. 2009; 66–70.
55. Yang L, Jelsbak L, Marvig RL, Damkiær S, Workman CT, Rau MH, et al. Evolutionary dynamics of bacteria in a human host environment. Proc Natl Acad Sci. 2011; 7481–7486.
56. Smith EE, Buckley DG, Wu Z, Saenphimmachak C, Hoffman LR, D'Argenio DA, et al. Genetic adaptation by Pseudomonas aeruginosa to the airways of cystic fibrosis patients. Proc Natl Acad Sci U S A. 2006; 8487–92.
57. Woo TE, Duong J, Jervis NM, Rabin HR, Parkins MD, Storey DG, et al. Virulence adaptations of Pseudomonas aeruginosa isolated from patients with non-cystic fibrosis bronchiectasis. Microbiology. 2016; 2126–2135.
58. Feltner JB, Wolter DJ, Pope CE, Groleau MC, Smalley NE, Greenberg EP, et al. LasR variant cystic fibrosis isolates reveal an adaptable quorum-sensing hierarchy in Pseudomonas aeruginosa. MBio. 2016; 1–9.
59. Sandoz KM, Mitzimberg SM, Schuster M. Social cheating in Pseudomonas aeruginosa quorum sensing. Proc Natl Acad Sci. 2007; 15876–15881.
60. Folkesson A, Jelsbak L, Yang L, Johansen HK, Ciofu O, Høiby N, et al. Adaptation of Pseudomonas aeruginosa to the cystic fibrosis airway: an evolutionary perspective. Nat Rev Microbiol. 2012; 841–51.
61. O'Brien S, Williams D, Fothergill JL, Paterson S, Winstanley C, Brockhurst MA. High virulence sub-populations in Pseudomonas aeruginosa long-term cystic fibrosis airway infections. BMC Microbiol. 2017; 30.

814 62. Mowat E, Paterson S, Fothergill JL, Wright EA, Ledson MJ, Walshaw MJ, et al.
815 Pseudomonas aeruginosa population diversity and turnover in cystic fibrosis chronic
816 infections. Am J Respir Crit Care Med. 2011; 1674–1679.
817 63. Peleg AY, Hooper DC. Hospital Acquired Infections Due to Gram-Negative Bacteria. N
818 Engl J Med. 2011; 1804–1813.
819 64. Gaynes R, Edwards JR. Overview of nosocomial infections caused by gram-negative
820 bacilli. Clin Infect Dis. 2005; 848–854.
821 65. Cosgrove SE, Carmeli Y. The Impact of Antimicrobial Resistance on Health and Economic
822 Outcomes. Clin Infect Dis. 2003; 1433–1437.
823 66. Stiernagle T. Maintenance of C. elegans. WormBook : the online review of C. elegans
824 biology. WormBook. 2006.
825 67. Rasband WS. ImageJ. 1997.
826 68. Savoia D, Zucca M. Clinical and environmental Burkholderia Strains: Biofilm production
827 and intracellular survival. Curr Microbiol. 2007; 440–444.
828 69. Langmead B, Salzberg SL. Fast gapped-read alignment with Bowtie 2. Nat Methods. 2012;
829 357–360.
830 70. Li H. A statistical framework for SNP calling, mutation discovery, association mapping and
831 population genetical parameter estimation from sequencing data. Bioinformatics. 2011;
832 2987–2993.
833 71. Cingolani P, Platts A, Wang LL, Coon M, Nguyen T, Wang L, et al. A program for
834 annotating and predicting the effects of single nucleotide polymorphisms, SnpEff: SNPs in
835 the genome of Drosophila melanogaster strain w 1118; iso-2; iso-3. Fly. 2012; 80–92.
836 72. R Development Core Team. R: A language and environment for statistical computing. R
837 Foundation for Statistical Computing. 2016.
838 73. Hadfield JD. MCMC methods for multi-response generalized linear mixed models: The
839 MCMCglmm R package. J Stat Softw. 2010; 1–22.
840 74. Le S, Josse J, Husson F. FactoMineR: An R Package for Multivariate Analysis. J Stat Softw.
841 2008; 1–18.
842

SUPPLEMENTARY MATERIAL

Figures S1-S5

Tables S1-S3